Supporting Information

Efficient Photochemical Oxygen Generation from Water by a Phosphorus-doped H_2MoO_5

Qing Kang,[a] Zhongwei Mei,[b, c] Tao Wang,[a] Kun Chang,[a] Lequan Liu,[a] and Jinhua Ye[a, b, c, d*]

[a] *International Center for Materials Nanoarchitectonics (MANA), National Institute for Materials Science (NIMS), 1-1 Namiki, Tsukuba, Ibaraki 305-0044, Japan.*

[b] *Catalytic Materials Group, Research Unit for Environmental Remediation Materials, National Institute for Materials Science (NIMS), 1-1 Namiki, Tsukuba, Ibaraki 305-0044, Japan.*

[c] *Graduate School of Chemical Science and Engineering, Hokkaido University, Sapporo, Japan*

[d] *TU-NIMS Joint Research Center, School of Materials Science and Engineering, Tianjin University, 92 Weijin Road, Nankai District, Tianjin 300072, P. R. China*

[*] Corresponding author E-mail: Jinhua.YE@nims.go.jp

Experimental Details

Chemicals and materials

MoO_3 (≥99.8% purity), H_2O_2, H_3PO_4, $AgNO_3$, WO_3, and $(NH_4)_{10}W_{12}O_{41}$ were purchased from Wako (Japan) and other reagents of analytical reagent grade were all obtained from commercial sources and used as received. Twice distilled water was used throughout the experiments.

Sample synthesis

In a typical synthetic procedure of P-doped and undoped H_2MoO_5 powders, 3 g of MoO_3 was thoroughly mixed with 30 mL aqueous solution containing appropriate amounts of H_3PO_4. Few H_2O_2 was added into the resulting solution to prevent the reduction of Mo^{6+}. After condensing at 373 K for 3 hours, the solution was filtered in order to remove any precipitates. Then the filtrate was concentrated by evaporation and dried at 373 K for 17 hours in air. Yellow crystalline products were obtained. The samples were denoted as P_xMo_y, where x, y represents the molar ratio of phosphorus and molybdenum in precursor solution. Undoped H_2MoO_5 was obtained in the same way but without adding H_3PO_4 solution.

WO_3 powder were purchased from Wako (Japan) or synthesized as previous reported[1]. A certain amount of $(NH_4)_{10}W_{12}O_{41}$ and 200 mL water were heated to 353 K and stirred for 2 hours, yielding a clear solution. After evaporation of the water, the remaining slurry was dried at 383 K for 6 hours followed by calcination at 873 K for another 6 hours in air.

Physicochemical characterization

The crystal structures were determined X-ray diffractometer (XRD, RINT 2000; Rigaku Corp.) employing Cu Kα radiation (λ = 1.54178 Å). The FTIR spectra were collected with a BIORAD FTS 6000 FTIR spectrometer, equipped with an attenuated total reflection (ATR) setup. Before FTIR test, all samples were dehydrated at 100 ^oC for 17 hours to make sure the same dehydration degree. X-ray Photoelectron Spectroscopy (XPS) experiments were performed in a Theta probe (Thermo Fisher) using monochromatic Al Kα X-rays at hυ = 1486.6 eV. Peak positions were internally referenced to the C_{1s} peak at 284.6 eV. The ultraviolet-visible diffuse reflectance spectra were measured using the diffuse reflection method with a Shimadzu UV-2500 spectrophotometer. Then the absorption spectra were obtained from the reflectance spectra by means of Kubelka-Munk transformations. The contact angle measurements were tested on DropMaster 300 (Japan). Sample morphologies were studied using a field-emission scanning electron microscope (FE-SEM, S-4800, Hitachi Instrument). Specific surface area of samples was measured by the BET method (N_2 adsorption) with a Gemini-2360 instrument (Micrometrics, Shimadzu).

Oxygen evolution and quantum efficiency

The photochemical activities under visible light illumination were investigated by measuring O_2 evolution at room temperature under atmospheric pressure in a closed pyrex glass vessel (405 ml)

containing nitrogen purged suspension of 0.05~0.5 g sample powder in 255 mL aqueous solution. $AgNO_3$ (0.85 g) or $Ce(SO_4)_2$ (2.02 g) was added in the experiments involving sacrificial reagent. The pH values of the solution were modulated by diluent NaOH or HNO_3. The light source was an ozone-free 300 W Xe arc lamp (Hayashi Tokei, Luminar Ace 210). A cutoff filter of 420 nm was employed for the visible-light irradiation. The light intensity was measured by a spectroradiometer (Ushio, USR-40). The quantum efficiency at various wavelengths was measured by inserting a water filter and various band-pass filters in front of the reaction cell to get the desired incident wavelength. At the same time, the light intensity was tuned to minimize diffusive reflection of the incident light. The amount of evolved O_2 was determined using a gas chromatograph (Shimadzu, GC-8A, TCD, Ar carrier) and the quantum efficiency was obtained from the percentage of the number of reacted electrons during O_2 evolution to the number of incident photons. Electrical resistance measurements were tested by pressing equal powder samples into discs with same areas and measuring the electrical resistance by Keithley 2400 sourcemeter (USA).

Characterization of Photoinduced Hydrophilicity

The P-doped H_2MoO_5 thin film was prepared by the spin-coating technique. In a typical process, P_3Mo_{12} sample was prepared to be a sol-gel in acetone-water. The pH value of the sol-gel was adjusted to 1~7. The sol-gel was spin-coated on ITO substrates with a rate of 1000 rpm for 10 s. This process was repeated for 20 times. Then the thin film was dried at 303 K overnight. After visible light irradiation for 10 min, the measurements of contact angle were performed. Five different positions on one film were tested. The highest and lowest values of contact angle were ignored, and the other values were used to calculate the average.

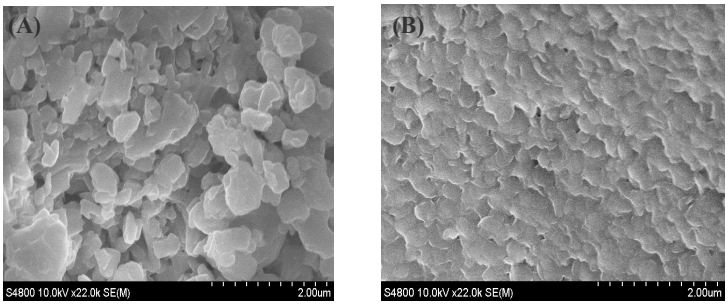

Figure S1. FESEM images of undoped (A) and P-doped (B) H_2MoO_5.

Figure S1 shows the changes in the surface morphology of H_2MoO_5 before and after phosphorus-doping (P-doping) observed by FESEM. The block structure of undoped H_2MoO_5 disappeared after P-doping. The doped sample exhibited smooth surface and monodisperse fine particles ~ 200 nm on average in size, which was considerably smaller than the particle size of the undoped sample. This is due to surface dissolution of the H_2MoO_5 caused by the small amount of phosphate. Note that the particle sizes estimated by FESEM observation are larger than the crystallite sizes presented in Table S2 owing to possible formation of secondary particles. As shown in Table S2, the P-doped H_2MoO_5 samples have lower specific surface areas than undoped H_2MoO_5. This is consistent with the lack of mesoporous in the P-doped H_2MoO_5 sample, as observed in FESEM image.

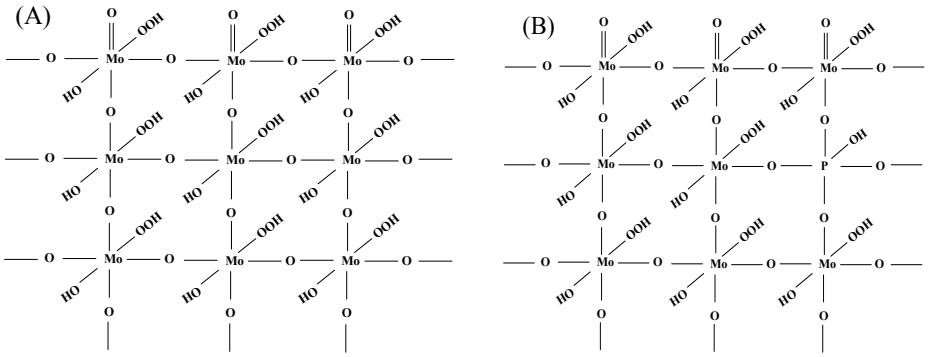

Figure S2. Scheme of undoped (A) and P-doped (B) H_2MoO_5.

The concentration of P element in P_3Mo_{12} sample was determined by XPS and ICP-OES. As shown in Figure 1C and Table S1, the P in P_3Mo_{12} sample is 1.92 wt% determined by XPS and 2.74 wt% by ICP. Considering XPS can only characterize the surface property of P_3Mo_{12} and ICP can determine the total P concentration in bulk sample, we calculated that ~70% P is existing in the form of amorphous POx or interstitial P doping and ~30% P is in the form of Mo-O-P.

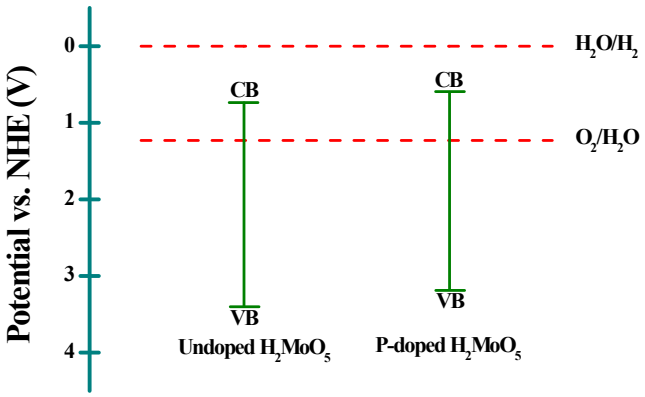

Figure S3. Schematic illustration of the band potentials of undoped and P-doped H_2MoO_5.

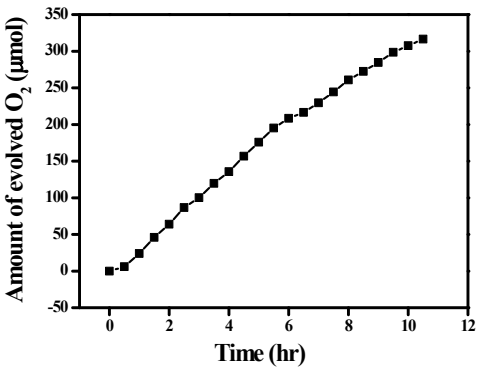

Figure S4. Long time measurements of O_2 evolution from aqueous $AgNO_3$ solution (pH4) over P-doped H_2MoO_5 under visible light illumination.

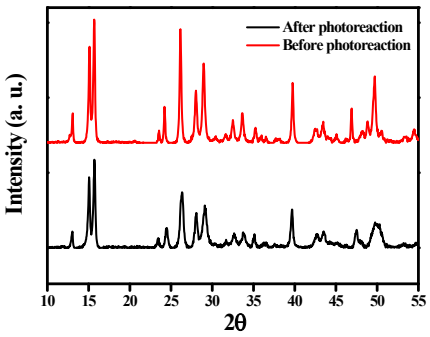

Figure S5. XRD of P-doped H_2MoO_5 samples.

The vitality and stability of the P-doped H_2MoO_5 is shown in Figure S4 and Figure S5, respectively. After ten hours visible light illumination, the O_2 evolution performance on P-doped H_2MoO_5 sample does not show any detectable descent (Figure S4). This indicates the high vitality of the P-doped H_2MoO_5. And after the photochemical reaction, although some descent in XRD intensity due to the solution of the sample, none of segregated impurity phase is involved (Figure S5), indicating the high stability of the P-doped H_2MoO_5.

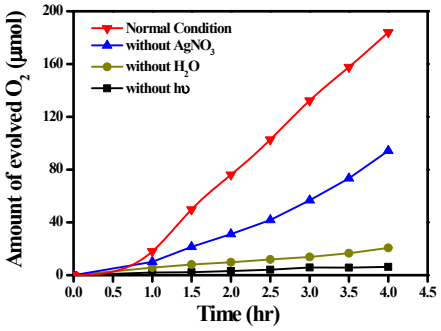

Figure S6. Control experiments over P-doped H_2MoO_5.

Figure S6 further confirms that O_2 evolution over P-doped H_2MoO_5 is derived from photochemical water oxidation. Without visible light illumination negligible O_2 evaluated. This means the oxygen evolution is motivated by light. To confirm the oxygen observed is not derived from the decomposition of P-doped H_2MoO_5 sample, control experiment without H_2O was carried out on irradiated P-doped H_2MoO_5 sample. Little O_2 was evaluated in four hour visible light irradiation and once we add H_2O (without $AgNO_3$) into the reaction cell obvious O_2 evolution was observed. These results indicate the above observed oxygen is indeed come from the oxidation of water.

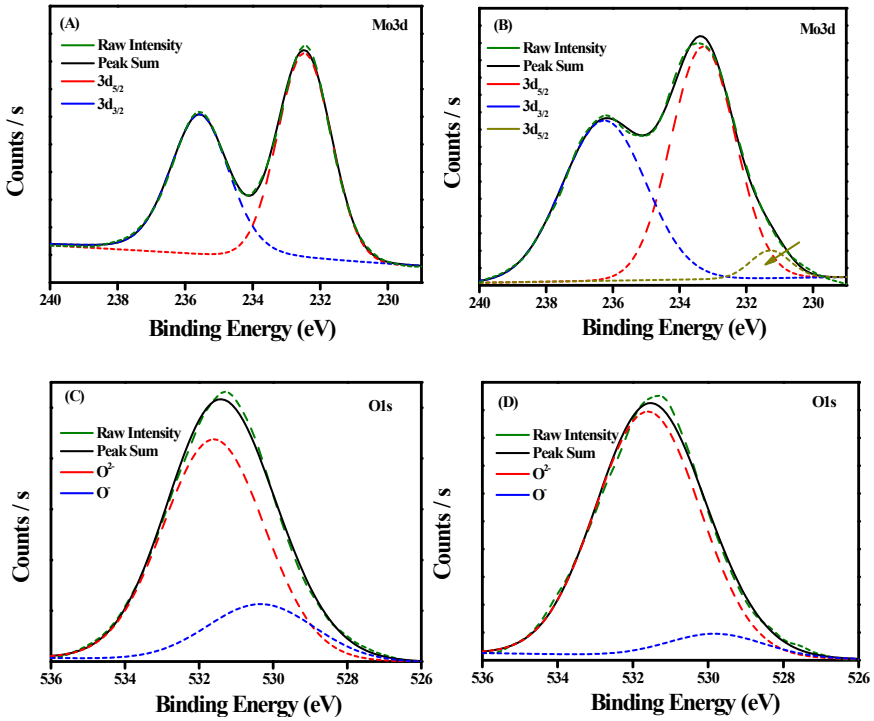

Figure S7. XPS spectra of P-doped H_2MoO_5 before (a, c) and after (b, d) photoreaction without $AgNO_3$.

Figure S7 shows Mo3d and O1s XPS spectra changes of P-doped H_2MoO_5 sample before and after photoreaction without sacrificial reagent. After the photoreaction a new Mo3d5/2 peak emerges, which is attributed to characteristic Mo^{5+} peak, and the O^- peak greatly decreased.[2] This indicates that the photogenerated electrons are consumed by Mo^{6+} and O^-, while the photogenerated holes produce oxygen evolution when the reaction system doesn't contain any sacrificial reagent.

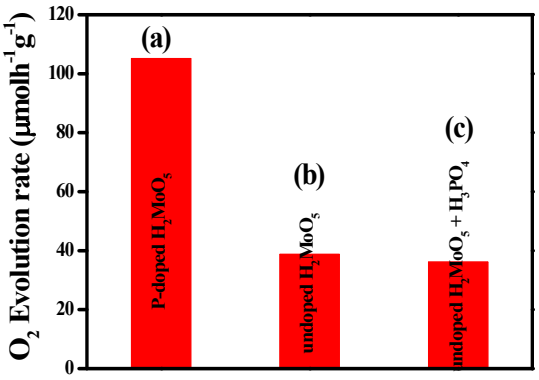

Figure S8. O_2 evolution rate over P-doped H_2MoO_5 (a) and undoped H_2MoO_5 (b, c) from aqueous $AgNO_3$ solution (pH 4) or (c) equivalent amount of H_3PO_4 was added.

Since the presence of phosphate in the synthesis process of H_2MoO_5, one might suspect that Ag_3PO_4 originating from silver ion in solution may contribute to the high activity. However, this possibility is excluded by the control photochemical reaction: with or without an equivalent amount of phosphate acid intentionally added into the reaction solution containing silver nitride, the O_2 evolution rates are not much different (Figure S8). Accordingly, it is reasonable to attribute the enhanced photochemical activity on P-doped H_2MoO_5 to the changes of the inherent properties of H_2MoO_5.

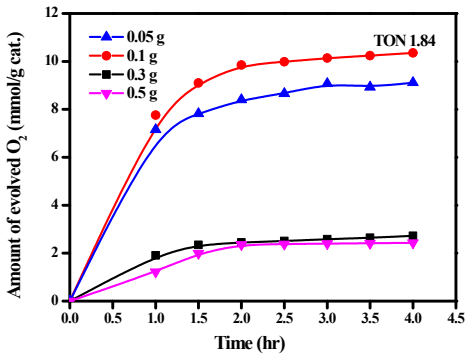

Figure S9. Effect of the amount of P_3Mo_{12} on O_2 evolution performance.

The amount of P_3Mo_{12} sample is optimized in Figure S9. In our case, the 0.1 g P_3Mo_{12} is enough for the water oxidation and the calculated highest turnover number (TON) and turnover frequency (TOF) are 1.84 and 1.38 h^{-1}, respectively.

Table S1 ICP-OES Determination characterization for P and Mo elements

Sample	Initially molar ratio of P:Mo	Element (wt %)	
		P	Mo
$\mathbf{P_1Mo_{36}}$	1:36	0.31±0.01[a]	54.2±0.2[a]
		0.30±0.02[b]	54.0±0.1[b]
$\mathbf{P_1Mo_{12}}$	1:12	1.08±0.01[a]	52.5±0.2[a]
		1.04±0.02[b]	53.5±0.1[b]
$\mathbf{P_3Mo_{12}}$	3:12	2.74±0.01[a]	49.3±0.1[a]
		2.80±0.01[b]	48.9±0.1[b]
$\mathbf{P_6Mo_{12}}$	6:12	6.11±0.01[a]	46.5±0.3[a]
		6.08±0.01[b]	46.2±0.1[b]

[a] ICP analysis of the P-doped H_2MoO_5 before photoreactions.

[b] ICP analysis of the P-doped H_2MoO_5 after photoreactions.

Table S2 Summary of the physicochemical properties of the prepared samples

Samples	Spacing d[a] (nm)	Crystallite size[b] (nm)	S_{BET}[c] (m^2/g)
H_2MoO_5	0.2270	65.0	8.89
P_1Mo_{36}	0.2268	66.2	7.46
P_3Mo_{12}	0.2266	69.3	5.14
P_6Mo_{12}	0.2260	56.1	5.81

[a] Calculated by the Bragg formula according to the (30**Error!**) peaks located at 2θ = 39.0-40.5°

[b] Calculated by the Scherrer formula according to the (30**Error!**) peaks located at 2θ = 39.0-40.5°

[c] BET surface area calculated from the linear part of the BET plot

References

1 A. Ulgen and W. Hoelderich, *Catalysis Letters*, 2009, **131**, 122.

2 F. S. Hoor, C. Tharamani, M. Ahmed and S. Mayanna, *J. Power Sources*, 2007, **167**, 18.